Dental Materials 40 (2024) 1507–1514

Contents lists available at ScienceDirect

Dental Materials

journal homepage: www.elsevier.com/locate/dental

Physicochemical characterization of experimental resin-based materials containing calcium orthophosphates or calcium silicate

Mariana C.A. Resende [a], Handially S. Vilela [a], Marina D.S. Chiari [a], Rafael B. Trinca [a], Flávia R.O. Silva [b], Roberto R. Braga [a,*]

[a] Department of Biomaterials and Oral Biology, School of Dentistry, University of São Paulo, São Paulo, Brazil
[b] Institute of Energy and Nuclear Research, University of São Paulo, São Paulo, Brazil

ARTICLE INFO

Keywords:
Resin materials
Calcium orthophosphate
Calcium silicate
Mechanical properties
Optical properties
Ion release

ABSTRACT

Objective: To evaluate experimental dimethacrylate-based materials containing calcium orthophosphates or calcium silicate particles in terms of their optical, mechanical and Ca^{2+} release behaviour.
Methods: Dicalcium phosphate dihydrate (DCPD), hydroxyapatite (HAp), beta-tricalcium phosphate (β-TCP) or calcium silicate (CaSi) particles were added to a photocurable BisGMA/TEGDMA resin (1:1 in mols) at a 30 vol% fraction. Materials containing silanized or non-silanized barium glass particles were used as controls. Degree of conversion (DC) at the top and base of 2-mm thick specimens was determined by ATR-FTIR spectroscopy ($n = 5$). Translucency parameter (TP) and transmittance (%T) were determined using a spectrophotometer ($n = 3$). Biaxial flexural strength (BFS) and flexural modulus (FM) were determined by biaxial flexural testing after 24 h storage in water ($n = 10$). Ca^{2+} release in water was determined during 28 days by inductively coupled plasma optical emission spectrometry ($n = 3$). Statistical analysis was performed using ANOVA/Tukey test (DC: two-way; TP, %T; BFS and FM: one-way; Ca^{2+} release: repeated measures two-way, $\alpha = 5$ %). *Results:* CaSi and β-TCP particles drastically reduced DC at 2 mm, TP and %T ($p < 0.001$). Compared to both controls, all Ca^{2+}-releasing materials presented lower BFS ($p < 0.001$) and only the material with DCPD showed significantly lower FM ($p < 0.05$). The material containing CaSi presented the highest Ca^{2+} release, while among materials formulated with calcium orthophosphates the use of DCPD resulted in the highest release ($p < 0.001$).
Significance: CaSi particles allowed the highest Ca^{2+} release. Notwithstanding, the use of DCPD resulted in a material with the best compromise between optical behaviour, DC, strength and Ca^{2+} release.

1. Introduction

Resin-based composites have mechanical and optical characteristics that make them suitable to a broad range of indications in restorative dentistry. The annual failure rate (AFR) of composite restorations in posterior teeth placed under ideal conditions of operator skill and patient compliance is between 1.1 % to 2.5 % [1,2]. However, in high caries risk patients AFR is three times higher than the AFR registered for low caries risk patients [3]. The interest in functional resin composites containing calcium-releasing particles (*e.g.*, calcium orthophosphate particles, calcium silicates or bioactive glasses) has increased considerably in recent years, as an approach to slow down the progression of caries lesions [4]. These materials were shown to reduce bacterial activity and promote mineral precipitation in enamel and dentin, postponing the development of new lesions [5–10].

Differently from the silanized glass particles found in conventional composites, ion-releasing particles are not chemically bonded to the polymer matrix. Consequently, the mechanical performance of functional materials may be compromised due to inefficient stress distribution between both phases [11] and limited toughening effect [12]. Also, the lack of a sealed interface between particles and the polymer increases water sorption, accelerating hydrolytic degradation [13]. Finally, the mismatch between the refractive index (RI) of the resin matrix and the particles may lower the light transmittance through the material, reducing depth of cure and compromising restoration aesthetics [14]. Ideally, ion-releasing particles should present characteristics such as small size, high surface area, and RI compatible with the other constituents in order to minimize their negative impact on

* Correspondence to: Departamento de Biomateriais e Biologia Oral Faculdade de Odontologia da Universidade de São Paulo, Av. Prof. Lineu Prestes, 2227, São Paulo, SP 05508-000, Brazil.
E-mail address: rrbraga@usp.br (R.R. Braga).

https://doi.org/10.1016/j.dental.2024.07.002
Received 31 January 2024; Received in revised form 10 July 2024; Accepted 12 July 2024
Available online 23 July 2024

material's mechanical/optical behaviour. Concomitantly, their solubility should allow for optimal bioactivity without compromising the material's long-term durability.

Calcium orthophosphates are a large group of compounds with different crystalline structures (with the exception of amorphous calcium phosphate, ACP), solubilities (defined by their Ca/P ratio) and refractive indices [15]. Among them, dicalcium phosphate dihydrate (DCPD, $CaHPO_4{\cdot}2H_2O$, Ca/P = 1.0) has been tested as calcium source in resin-based materials due to its high solubility in comparison to other CaP phases (pK_s = 6.59) and RI (1.54–1.55) similar to barium glass (1.53) [15–17]. Hydroxyapatite particles (HAp, $Ca_{10}(PO_4)_6(OH)_2$, Ca/P = 1.67) has also been tested both as reinforcing and functional fillers in composites [18]. However, its RI (1.64–1.66) may result in a relatively opaque material [19]. Also, its low solubility in neutral conditions (pK_s = 116.8) may impair ion release, when compared to other calcium sources. β-tricalcium phosphate (β-TCP, $Ca_3(PO_4)_2$, Ca/P = 1.5, pK_s = 28.9) has an intermediate solubility between DCPD and HAp and, to the best of our knowledge, has not been tested as functional filler in resin composites.

Calcium silicates (CaSi, pK_s = 6–13 [20]) have been successfully used in Restorative Dentistry and Endodontics in the last few decades. Used as pulp capping materials, they upregulate odontoblastic activity and provide Ca^{2+} for mineral precipitation. Also, the release of hydroxyl ions promotes local alkalinisation, which favours apatite precipitation [21]. Though resin-based materials containing CaSi particles are commercially available [22], there are very few reports on the physicochemical characteristics of this particular association [23–25].

In general, studies evaluating experimental formulations focus on a single particle composition, varying its size [13] or the ratio between ion-releasing particles and reinforcing glass [12,26,27]. There are no studies comparing materials formulated with different calcium orthophosphate phases or materials containing calcium orthophosphates and calcium silicate. Therefore, the objective of this study was to evaluate the behaviour of experimental resin-based materials containing different calcium orthophosphate phases (DCPD, HAp, or β-TCP) and CaSi particles. The null hypothesis tested was that mechanical and optical characteristics, as well as Ca^{2+} release are not affected by the particle used in the formulation.

2. Materials and methods

2.1. Particles synthesis and characterization

Calcium orthophosphate particles (DCPD, HAp and β-TCP) were synthesized by precipitation, as described in the Supplementary material file. Calcium silicate particles were synthesized by a sol-gel method using a surfactant template (see Supplementary material). DCPD and HAp particles were milled (Qualification Micronizer Jet Mill, Sturtevant Inc., Hanover, MA, USA) in order to reduce their median size and narrow size distribution. All particles were characterized by x-ray diffraction (XRD, D2 Phaser, Bruker, Bremen, Germany). Diffractograms were obtained using Nickel filtered Cu Kα radiation at 40 kV and 30 mA. The geometry of the equipment was θ/2θ and reading was performed continuously from 10° to 60° at 2° per minute interval. Diffractograms were imported to Match! software (Crystal Impact, Redmond, WA, USA) for identification of the obtained phases. Particle size distribution was determined by laser light scattering (Mastersizer 2000, Malvern Instruments Ltd., Malvern, UK). Samples were sonicated in water for 1 min before being injected in the equipment. Refractive indices values used for particles and dispersant were 1.54 and 1.33, respectively. Size range was between 20 nm to 2000 μm. Particle morphology was observed under scanning electron microscopy (Quanta 650 FEG, Thermo Fisher, Waltham, MA, USA). Particle density was determined by helium pycnometry (Quantachrome, model Ultrapyc1200e, Boynton Beach, FL, USA). Silanized and non-silanized barium glass particles used in the control formulations (SDI Ltd, Bayswater, VIC, Australia) were also characterized.

2.2. Formulation of the experimental materials

Six materials were manipulated with the organic matrix containing BisGMA (bisphenol-A glycidyl dimethacrylate) and TEGDMA (triethylene glycol dimethacrylate) at equimolar ratio, plus 0.5 % by mass of photoinitiator (camphorquinone) and co-initiator (tertiary amine - N, N-dimethyl-4-ethyl aminobenzoate, EDMAB; all chemicals from Sigma-Aldrich, St. Louis, MO, USA). All materials were formulated with inorganic fraction of 30 vol%, defined as the maximum volume of CaSi capable of being incorporated into the resin matrix. As controls, materials containing 30 vol% of silanized or non-silanized barium glass particles (SDI Ltd, Bayswater, VIC, Australia) were used. The materials were mechanically mixed under vacuum (Speedmixer DAC150.1 FVZ-K, FlackTek Inc., Landrum, SC, USA) and kept under refrigeration up to two hours before use.

2.3. Optical properties

Fragments of fractured specimens in the biaxial flexural test (see item 2.5) with 1.2 mm in thickness (n = 3) were analysed in a spectrophotometer (CM-3700d, Konica Minolta, Tokyo, Japan), with the use of OnColorTM QC Lite software (CyberChrome Color Systems, Stone Ridge, NY, USA). The translucency parameter (TP) was calculated based on the CIEL*a*b* coordinates values obtained between 360 and 740 nm (at 10 nm intervals) with the standard D65 illuminant and a 8° viewing angle, using the following equation:

$$TP = \left[(L*B - L*W)^2 + (a*B - a*W)^2 + (b*B - b*W)^2 \right]^{1/2}$$

where L*B is luminosity on a black background, L*W is luminosity on a white background, a*B is chromatic along the green red axis on a black background, a*W is chromatic along the red-green axis on a white background, b*B is chromatic along the yellow-blue axis on black background and b*W the chromaticity along the yellow-blue axis on white background [28]. For transmittance (%T), samples were exposed to a light emission between 360 nm and 740 nm and the value corresponding to the 468 nm was recorded.

2.4. Degree of conversion

Degree of conversion (DC) was obtained by mid-infrared spectroscopy (Vertex 70, Bruker Optics, Ettlingen, Germany) using a total attenuated reflectance accessory (ATR-FTIR, Miracle, Pike Technologies, Inc., Madison, WI, USA). The non-polymerized material was inserted into a 2-mm thick square-shaped silicone mold (2 ×2 mm; n = 5) and a spectrum was obtained (32 scans, 4 cm^{-1} resolution). With the sample on the ATR crystal, the top surface was photoactivated (1300 mW/cm^2 for 20 s, Bluephase, Ivoclar Vivadent, Schaan, Liechtenstein) and a second spectrum was obtained after 30 min, corresponding to the specimen's non-irradiated (bottom) surface. Then, the specimen was inverted and pressed against the crystal to obtain the spectrum corresponding to the irradiated (top) surface. DC was calculated from the absorption band area ratio at 1610 cm^{-1} (aromatic absorption band) and 1640 cm^{-1} (aliphatic absorption band, C═C stretch), according to the formula:

$$DC = \left(1 - \frac{Ratio\_polymerized}{Ratio\_non\ polymerized}\right) x100$$

2.5. Mechanical properties

Discs (12 ×1.2 mm, n = 10) were made in a split steel matrix. Photoactivation was performed for 20 s on each quadrant of the specimen (Bluephase, Ivoclar Vivadent). After storage in deionized water for 24 h,

the specimen was tested on a "three spheres on a piston" device using a universal testing machine (Instron, model 5565, Instron Corp, Canton, MA, USA). The load was applied at the center of the specimen by means of a flattened piston with 1.2 mm diameter, at a crosshead speed of 0.5 mm/min. Deflection at the center of the disc was monitored by a transducer (model W-E401-E, Instron Corp.). The biaxial flexural strength (BFS, in MPa) was calculated using the equations below:

$$BFS = \frac{-0.2387 \quad P \quad (X - Y)}{h^2}$$

$$X = (1+\upsilon)\ln\left(\frac{r_2}{r_3}\right)^2 \quad + \left[\left(\frac{1-\upsilon}{2}\right) \quad\right] \quad \left(\frac{r_2}{r_3}\right)^2$$

$$Y = (1+\upsilon)\left[1 + \ln\left(\frac{r_1}{r_3}\right)^2 \quad\right] + (1-\upsilon) \quad \left(\frac{r_1}{r_3}\right)^2$$

where P is the fracture load (in Newtons); h is the thickness of the specimen (in mm); υ is the Poisson coefficient (0.24) [29]; r_1 is the radius of the support circle (5 mm); r_2 is the radius of the loading area (0.6 mm); r_3 is the radius of the specimen (in mm).

Flexural modulus (FM) was calculated according to the formula below:

$$FM = \frac{\beta P a^2}{w h^3} \times 0.001$$

where β is a constant related to the deflection of the disc in the central region (0.509), P corresponds to the applied load (in Newtons), a is the radius of the disc, w is the deflection corresponding to the load P and h is the thickness of the disc (all in mm).

2.6. Scanning electron microscopy

The surface of the specimens was sputter-coated with carbon and observed under a scanning electron microscope (Quanta 650 FEG, Thermo Fisher, Waltham, MA, USA). Energy-dispersive X-ray spectroscopy (EDX) (Quantax 4030 and XFlash 6–60, Bruker Optics, Ettlingen, Germany) was used to map calcium distribution on the specimen surface.

2.7. Calcium release

Discs (5 ×1 mm, n = 3) were made and dry stored for 24 h at 37 °C before their masses were determined on an analytical scale (Mettler Toledo, model XS105, Columbus, OH, USA). Specimens were immersed individually in 10 mL of ultrapure water. The immersion medium was changed weekly for four weeks and the solutions were filtered (pore size: 0.45 μm), acidified with 100 % nitric acid in the ratio 1 μl of acid: 1 mL of solution, and analysed by inductively coupled plasma optical emission spectrometry (ICP-OES, Agilent Technologies, Santa Clara, CA, USA).

2.8. Statistical analysis

Data were normally distributed and homoscedastic and, therefore, analysed using two-way (DC) or one-way (optical properties and BFS/FM) analysis of variance (ANOVA). Repeated measures two-way ANOVA was used to analyse Ca^{2+} release data. In all cases, the Tukey test was used for multiple comparisons and the overall significance level was 5 %.

3. Results

3.1. Particles characterization

Particle phase identification is presented in the diffractograms (Appendix Fig. S1). The formation of DCPD, HAp and β-TCP were confirmed, while dicalcium silicate was the CaSi phase obtained in the sol-gel synthesis. Particle median (D_{50}), as well as D_{10}, D_{90} and the span ($D_{90} - D_{10}/D_{50}$) are presented in Table 1. Particle size distribution is shown in the Appendix (Fig. S2). HAp presented the largest D_{50} and a much broader distribution than the other particles, numerically expressed by the span value (4.4). The narrowest distributions were presented by the DCPD particles and by both barium glasses (span: 1.7 – 1.9). Particles morphologies are presented in Fig. 1. DCPD particles (Fig. 1A and B) show the characteristic flat plate aspect, with rounded corners. HAp particles (Fig. 1C and D) present irregular shape and rough surface. Under lower magnification it is possible to observe the large variation in sizes. β-TCP (Fig. 1E and F) and CaSi (Fig. 1G and H) are nanoparticles agglomerates. The variety of sizes observed for β-TCP agrees with its higher span value, in comparison to CaSi.

3.2. Optical properties

All materials containing Ca-releasing particles presented lower translucency parameter (TP) in comparison to the controls ($p < 0.001$, Fig. 2A), with more severe reductions for materials containing CaSi and β-TCP ($p < 0.001$). Materials with DCPD and HAp showed statistically similar TP. Transmittance (%T, at 468 nm) presented a similar pattern, except for the fact that the materials with DCPD and HAp reached statistically similar %T to both controls. Also, between the controls the material containing non-silanized glass presented statistically lower transmittance ($p < 0.001$, Fig. 2B). The translucency of the tested materials against a standardized background can be seen in the Appendix (Fig. S3).

3.3. Degree of conversion

"Material*depth" interaction was statistically significant ($p < 0.001$). There was no difference between the materials for degree of conversion (DC) determined on the irradiated surface. At 2 mm depth, however, all materials containing Ca-releasing particles showed statistically lower DC values than those recorded at the top surface. The reductions were particularly severe for materials with CaSi and β-TCP, where the "base-to-top" (B/T) ratios were respectively 0.1 and 0.2. For materials with DCPD and HAp, B/T ratios were higher (respectively, 0.8 and 0.7). No statistically significant reductions in DC between top and bottom surfaces were observed for the controls.

3.4. Mechanical properties

In comparison to the control containing silanized glass, all groups presented statistically lower biaxial flexural strength (BFS) values (Fig. 4A, $p < 0.001$). The materials containing HAp and β-TCP showed the lowest BFS, statistically similar to each other and representing only 26 % of the BFS reached by the material with silanized glass. The material with non-silanized glass particles presented BFS equivalent to 55 % of the composite containing silanized glass, while the BFS of the

Table 1
Particle size distribution parameters (D_{10}, D_{50}, D_{90}, in micrometers, and span, $D_{90} - D_{10}/D_{50}$) and refractive index of the particles used in the study.

Particles	D_{10}	D_{50}	D_{90}	Span	Refractive index
DCPD	2.4	6.7	13.9	1.7	1.54-1.55*
β -TCP	2.0	11.0	37.7	3.2	1.63*
HAp	3.1	27.8	126.2	4.4	1.64-1.66*
Ca_2SiO_4	2.2	8.4	24.0	2.6	1.71-1.73**
Silanized barium glass	0.5	0.9	2.0	1.7	1.53***
Non-silanized barium glass	0.6	1.8	4.0	1.9	1.53***

* http://www.handbookofmineralogy.org/.
** https://www.mindat.org/min-2333.html.
***Manufacturer information.

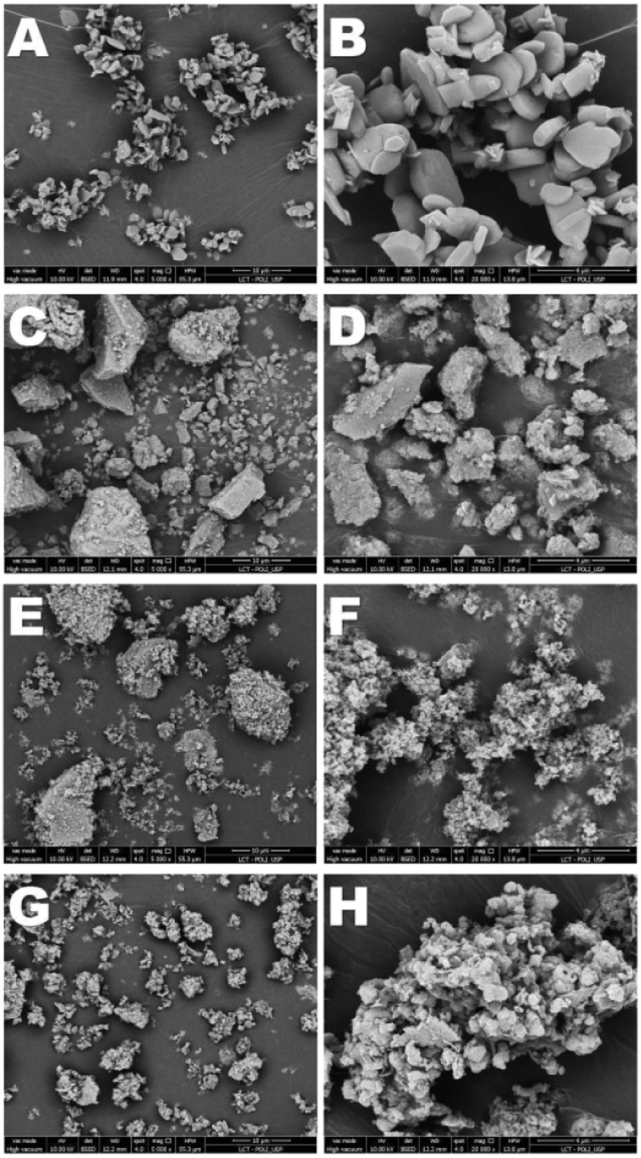

Fig. 1. Scanning electron microscopy images of the particles used in the formulations: DCPD (A and B), HAp (C and D), β-TCP (E and F) and CaSi (G and H).

material with DCPD corresponded to 37 % of the control composite. A regression analysis including the materials containing Ca-releasing materials and the material with non-silanized glass revealed an exponential decrease in BFS with the increase of the particle size D_{50} (Fig. 4B).

Flexural modulus (FM) was not affected by glass silanization (Fig. 4C). The materials containing CaSi and β-TCP also showed FM similar to the controls. The material with HAp presented the highest FM and the material with DCPD, the lowest FM among the tested materials ($p < 0.05$).

3.5. Scanning electron microscopy

All materials presented particles well dispersed in the polymer matrix (Fig. 5). Under lower magnification, the glass-filled materials and the material containing DCPD showed a more homogeneous microstructure due to their relatively small particle median size and narrow distribution, in comparison to materials containing HAp, β-TCP and CaSi. The EDX mapping for calcium revealed a more disperse distribution in materials containing DCPD and β-TCP, in comparison to HAp and CaSi.

3.6. Ion release

Ca^{2+} release over 28 days is shown in Fig. 6. Materials containing DCPD, HAp and β-TCP presented a steady release overtime, while the material containing CaSi presented a statistically significant reduction between 14 and 21 days ($p < 0.001$). After 28 days, the cumulative release was 466 μg/cm^2 (40.2 ppm) for CaSi, 212 μg/cm^2 (23.3 ppm) for DCPD, 64 μg/cm^2 (7.0 ppm) for HAp and 57 μg/cm^2 (6.3 ppm) for β-TCP.

4. Discussion

Particles used in the tested formulations differ in composition, morphology, size and solubility. The association of these characteristics determines their effect on the materials physicochemical behaviour. Therefore, the experimental resin-based materials tested in this study differed in their optical, mechanical and Ca^{2+}release behaviour, allowing the rejection of the null hypothesis.

The translucency parameter (TP) expresses the colour difference of a material when placed in contact with a black and a white backgrounds [30]. Transmittance (%T) expresses the percentage of incident light passing through a certain thickness of the material and is related to cure depth [31]. The materials containing CaSi and β-TCP presented very low TP and %T. Their optical behaviour can be attributed to refractive index (RI) mismatch between the resin matrix (RI: 1.50–1.56) and the particles [14]. Additionally, the fact that both particles are nanostructured agglomerates may have contributed to increase light scattering [32]. HAp, despite presenting RI close to that of β-TCP (1.64–1.66), resulted in a material with TP and %T similar to the material with DCPD (1.54–1.55). Possibly, its large particle size associated with the material's low inorganic content reduced light scattering [33], increasing translucency and transmittance. The statistically similar %T between the material formulated with DCPD and both materials containing barium glass confirms the findings of a previous study [34]. Interestingly, the material containing non-silanized glass showed reduced %T in relation to the composite with silanized glass, explained by the presence of gaps at the interface with the organic matrix increasing light dispersion [35].

Differences in optical parameters did not affect degree of conversion (DC) at the irradiated surface. In fact, previous studies using near-FTIR revealed a higher DC in 0.8 mm-thick specimens containing 30 vol% DCPD in comparison to a composite with 30 vol% glass particles [12]. However, all the ion-releasing materials presented statistically significant reductions in DC at 2-mm depth, which were particularly severe for materials containing CaSi and β-TCP as a result of their low %T. Materials containing DCPD and HAp also showed a statistically significant reduction in DC between top and base, consistent with their numerically lower %T registered in 1.2-mm thick specimens, in relation to glass-containing controls. In spite of the similar %T of the materials with HAp, DCPD and non-silanized glass, only the later showed statistically similar DC between top and 2-mm surfaces. Its lower viscosity and, consequently, greater mobility of the reactive species in relation to the materials with DCPD and HAp may explain this finding [36].

All formulations presented statistically lower biaxial flexural strength (BFS) in comparison to the material containing silanated glass, in agreement with previous studies [26,27,37,38]. The lack of a chemical bond between the particles and the polymer matrix hinders stress distribution between both phases, increasing the risk of crack initiation at relatively low loads [26]. Additionally, calcium orthophosphate particles present low cohesive resistance compared to glass [39]. Noteworthy, an exponential relationship between BFS and D_{50} was verified for materials formulated with non-bonded particles, regardless of their morphology and structure (i.e., nanoparticle agglomerates or non-porous). Larger particles increase stress concentration at the particle/matrix interface [40]. Also, non-bonded particles may act as flaws

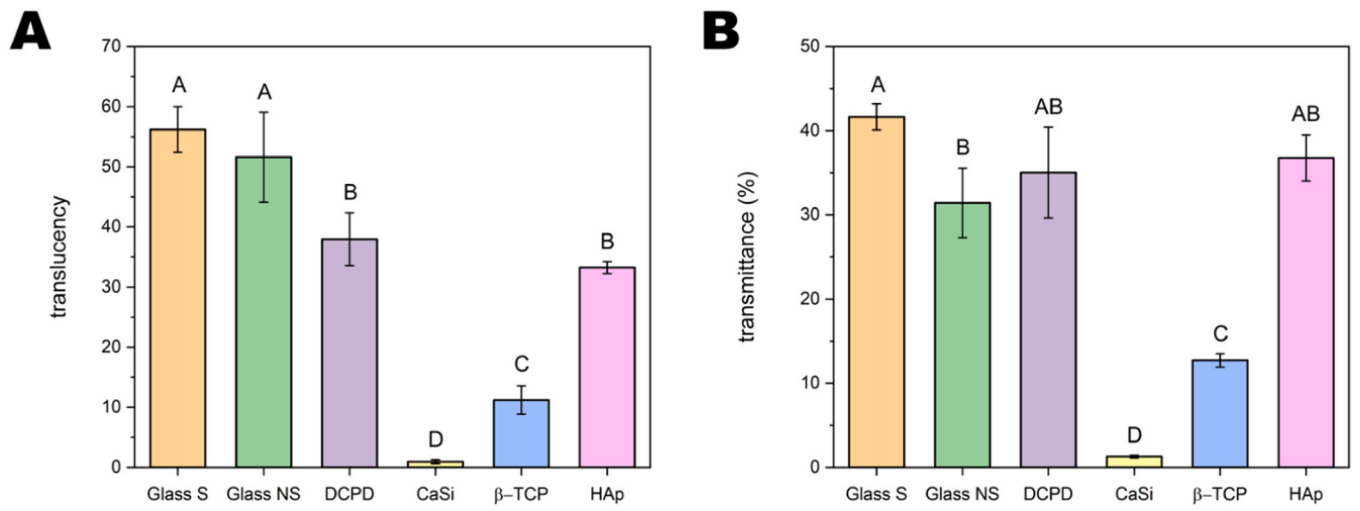

Fig. 2. Means and standard deviations for translucency (A) and transmittance (B), in %, of materials containing 30 vol% of particles. Different letters indicate a statistically significant difference between the groups (ANOVA 1 factor/Tukey test, $p < 0.05$).

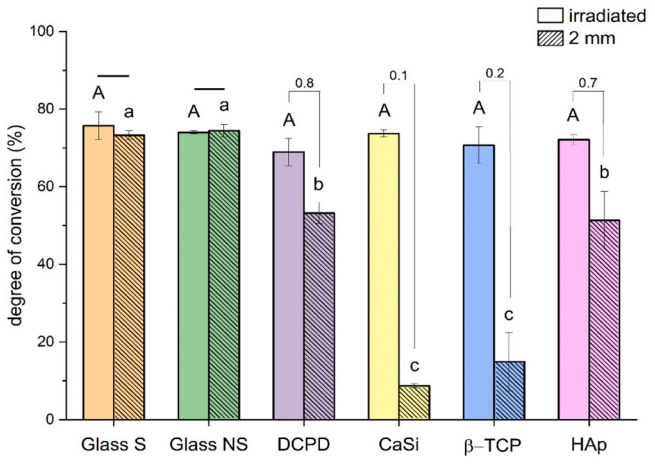

Fig. 3. Means and standard deviations for degree of conversion (in %). Similar upper-case letters indicate lack of statistically significant differences among materials at the irradiated surface. Similar lower-case letters indicate lack of statistically significant differences among materials at 2 mm from the irradiated surface. Lines connecting the bars indicate lack of statistically significant difference between the surfaces (two-way ANOVA/Tukey test, $p < 0.05$). Numbers above the brackets represent the DC "bottom-to-top" ratio.

and, according to Griffith's theory, strength is inversely proportional to the size of the crack initiating defect [41]. On the other hand, flexural modulus (FM) was not affected by the lack of chemical bond between particles, as verified in previous studies [26]. This property is related to the inter-particle interaction [42]. In fact, the material containing HAp particles, which shows the largest median and the broadest size distribution among the tested particles, presented the highest FM, in agreement with a previous study [43]. On the other hand, the lowest E value for the material with DCPD can be explained its narrow particle size distribution and flat-plate morphology, which may result in less particle interlocking compared to particles with irregular shape.

The percentage of calcium released from the specimens in relation to their Ca mass (i.e., fractional release) was small, also in agreement with previous investigations [12,44]. After 28 days, materials with HAp and β-TCP released, respectively, 1.5 % and 0.9 %. For materials with DCPD and CaSi, the percentages were higher (3.2 % and 6.3 %, respectively). Solubility and particle surface area explain the differences among materials. DCPD is more soluble than HAp at neutral pH [15], while the CaSi particles used in this study have porous structure, with high surface area, which increases the release [45]. Additionally, the calcium fraction in the CaSi crystalline structure is higher than in calcium orthophosphates (DCPD: 25.6 %, HAp: 39.9 %, β-TCP: 38.8 %, CaSi: 46.5 %). Finally, the β-TCP used in the study was synthesized in the presence of magnesium, which reduces its solubility, in spite of its high surface area [46]. There are fey few studies correlating Ca^{2+} release in solution with in vitro remineralization. For instance, a material containing anhydrous dibasic calcium phosphate (DCPA) and tetracalcium phosphate (TTCP)

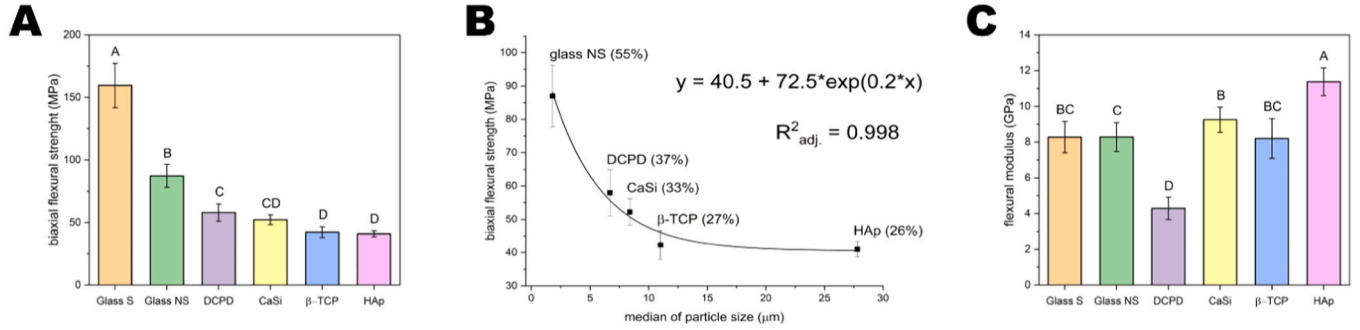

Fig. 4. (A) Averages and standard deviations for biaxial flexural strength (in MPa) of experimental materials. (B) Exponential regression between particle size median and biaxial flexural strength for materials containing non-bonded particles (percentages in parentheses indicate the BFS in relation to the material containing silanized glass). (C) Flexural modulus, in GPa. Different letters indicate a statistically significant difference (one-way ANOVA/Tukey test, $p < 0.05$).

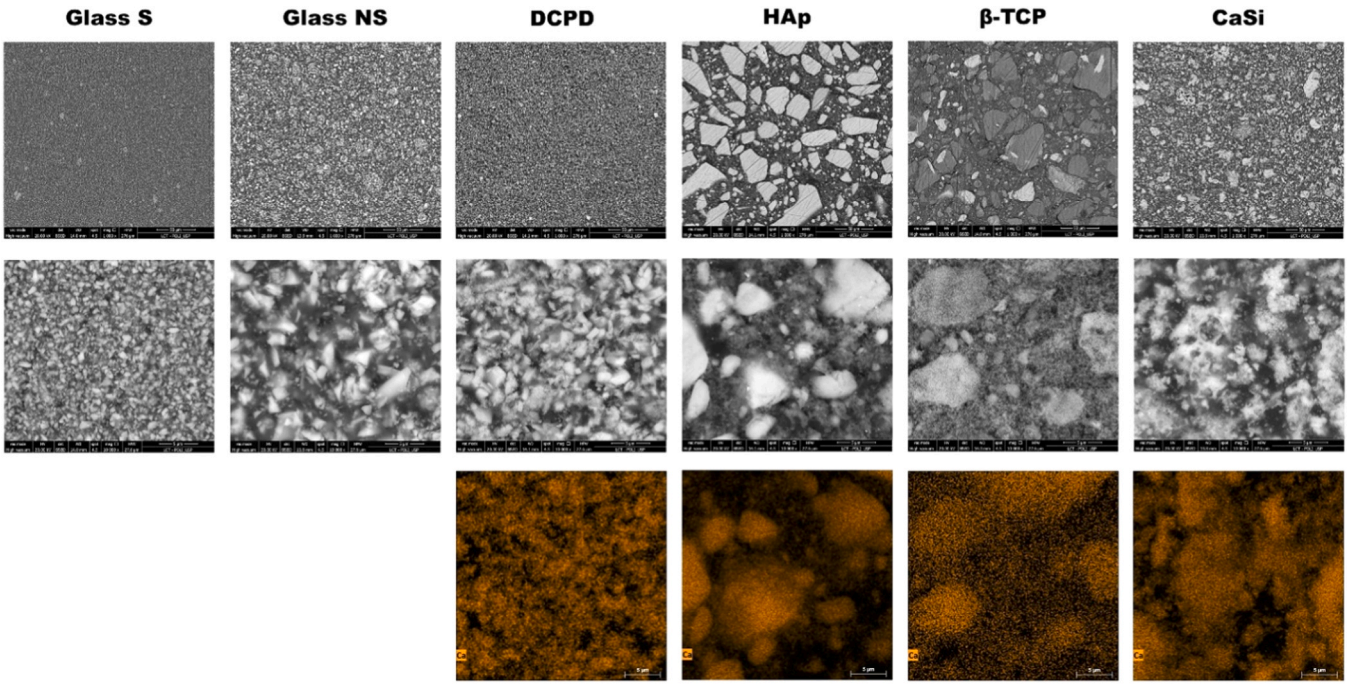

Fig. 5. Scanning electron microscopy images showing the microstructure of the tested materials (original magnifications, top row: 1000 x, middle row: 10,000 x). Bottom row: calcium mapping by energy-dispersive x-ray spectroscopy (EDX).

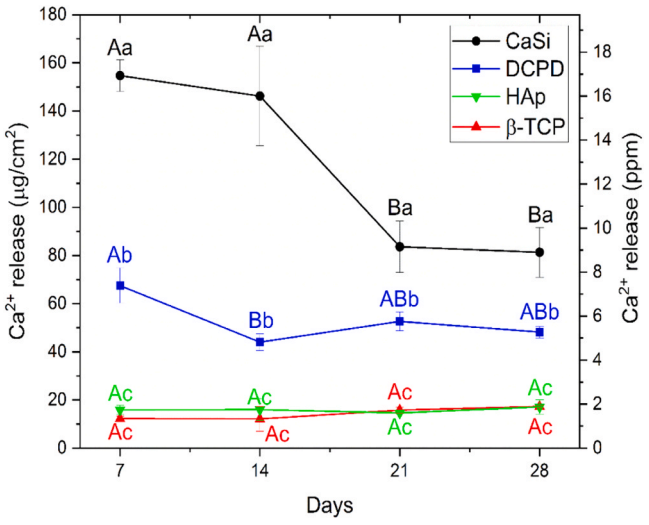

Fig. 6. Calcium release (left y-axis: μg/cm^2; right y-axis: parts per million) as a function of the immersion time in ultrapure water. Similar upper-case letters indicate lack of statistically significant differences for the same material in different periods. Similar lower-case letters indicate lack of statistically significant differences between materials at a given time (repeated measures two-way ANOVA, $p < 0.05$).

released 14 ppm of Ca^{2+} in 100 mL of artificial saliva over 42 days, which corresponded to a 38 % increase in mineral content of demineralized dentin samples [47]. Among the tested materials, only those formulated with CaSi (40.2 ppm) and DCPD (23.3 ppm) presented 28-days cumulative released concentrations above that. Future studies must focus on defining the limits (i.e., minimum and maximum Ca^{2+} release) necessary for achieving significant dentin remineralization. By doing so, formulations can be fine-tuned to optimize bioactivity, as well mechanical and optical properties. Also, considering the relative solubility of these particles, the materials' mechanical behaviour after long-term immersion in water and other solvents, as well as their wear resistance must be investigated in order to define if they can withstand being exposed to the oral environment.

5. Conclusion

Considering the limitations of the study, DCPD particles demonstrated to be an interesting choice for Ca^{2+} source in resin-based materials, as the resulting material presented [1] higher transmittance and degree of conversion than those formulated with β-TCP and CaSi and [2] higher fracture strength and Ca^{2+} release than materials with HAp and β-TCP. The only disadvantage of the material formulated with DCPD particles was the reduced flexural modulus. The null hypothesis can be rejected, as the materials containing Ca-releasing particles differed in all the tested characteristics.

Funding sources

This study was funded by the São Paulo Research Foundation (FAPESP), grants 2019/04737-4; 2020/12761-0; 2020/05986-5; 2022/08411-9.

CRediT authorship contribution statement

Mariana C.A. Resende: Investigation, Writing - Original draft, review & editing. **Handially S. Vilela**: Investigation, Writing - Review & editing. **Marina D.S. Chiari:** Investigation. **Rafael B. Trinca:** Investigation, Formal analysis. **Flávia R.O. Silva:** Investigation. **Roberto R. Braga:** Conceptualization, Supervision, Project administration, Formal analysis, Writing - review & editing.

Declaration of Competing Interest

None.

Acknowledgements

Authors would like to thank SDI for the donation of the barium glass

particles used in the study.

Appendix A. Supporting information

Supplementary data associated with this article can be found in the online version at doi:10.1016/j.dental.2024.07.002.

References

[1] Vetromilla BM, Opdam NJ, Leida FL, Sarkis-Onofre R, Demarco FF, van der Loo MPJ, et al. Treatment options for large posterior restorations: a systematic review and network meta-analysis. J Am Dent Assoc 2020;151(8):614–624 e18. https://doi.org/10.1016/j.adaj.2020.05.006.

[2] Da Rosa Rodolpho PA, Rodolfo B, Collares K, Correa MB, Demarco FF, Opdam NJM, et al. Clinical performance of posterior resin composite restorations after up to 33 years. Dent Mater 2022;38(4):680–8. https://doi.org/10.1016/j.dental.2022.02.009.

[3] Opdam NJ, van de Sande FH, Bronkhorst E, Cenci MS, Bottenberg P, Pallesen U, et al. Longevity of posterior composite restorations: a systematic review and meta-analysis. J Dent Res 2014;93(10):943–9. https://doi.org/10.1177/0022034514544217.

[4] Melo MAS, Garcia IM, Mokeem L, Weir MD, Xu HHK, Montoya C, et al. Developing bioactive dental resins for restorative dentistry. J Dent Res 2023;102(11):1180–90. https://doi.org/10.1177/00220345231182357.

[5] Ionescu AC, Degli Esposti L, Iafisco M, Brambilla E. Dental tissue remineralization by bioactive calcium phosphate nanoparticles formulations. Sci Rep 2022;12(1):5994. https://doi.org/10.1038/s41598-022-09787-5.

[6] Langhorst SE, O'Donnell JN, Skrtic D. In vitro remineralization of enamel by polymeric amorphous calcium phosphate composite: quantitative microradiographic study. Dent Mater 2009;25(7):884–91. https://doi.org/10.1016/j.dental.2009.01.094.

[7] Weir MD, Chow LC, Xu HH. Remineralization of demineralized enamel via calcium phosphate nanocomposite. J Dent Res 2012;91(10):979–84. https://doi.org/10.1177/0022034512458288.

[8] Melo MA, Weir MD, Rodrigues LK, Xu HH. Novel calcium phosphate nanocomposite with caries-inhibition in a human in situ model. Dent Mater 2013;29(2):231–40. https://doi.org/10.1016/j.dental.2012.10.010.

[9] Ionescu AC, Hahnel S, Chiari MDS, Konig A, Delvecchio P, Braga RR, et al. TEGDMA-functionalized dicalcium phosphate dihydrate resin-based composites prevent secondary caries in an in vitro biofilm model. J Funct Biomater 2022;13(4). https://doi.org/10.3390/jfb13040232.

[10] Thanyasiri S, Naruphontjirakul P, Padunglappisit C, Mirchandani B, Young AM, Panpisut P. Assessment of physical/mechanical properties and cytotoxicity of dual-cured resin cements containing Sr-bioactive glass nanoparticles and calcium phosphate. Dent Mater J 2023;42(6):806–17. https://doi.org/10.4012/dmj.2023-127.

[11] Fu S X-QF, Lauke B, Mai Y. Effects of particle size, particle/matrix interface adhesion and particle loading on mechanical properties of particulate–polymer composites. Compos B: Eng 2008;39(6):933–61.

[12] Campos AL, Vela BF, Pires Silva Borges L, Trinca RB, Pfeifer CS, Braga RR. Compositional boundaries for functional dental composites containing calcium orthophosphate particles. J Mech Behav Biomed Mater 2023;144:105928. https://doi.org/10.1016/j.jmbbm.2023.105928.

[13] Trinca RB, Oliveira BA, Vilela HDS, Braga RR. Effect of calcium orthophosphate particle size and CaP:glass ratio on optical, mechanical and physicochemical characteristics of experimental composites. Dent Mater 2023;39(9):770–8. https://doi.org/10.1016/j.dental.2023.06.012.

[14] Shortall AC, Palin WM, Burtscher P. Refractive index mismatch and monomer reactivity influence composite curing depth. J Dent Res 2008;87(1):84–8. https://doi.org/10.1177/154405910808700115.

[15] Dorozhkin SV. Calcium orthophosphates: occurrence, properties, biomineralization, pathological calcification and biomimetic applications. Biomatter 2011;1(2):121–64. https://doi.org/10.4161/biom.18790.

[16] Handbook of Mineralogy [Internet]. Mineralogical Society of America; 2003. Available from: ⟨http://www.handbookofmineralogy.org/⟩.

[17] Shortall AC, Palin WM, Burtscher P. Refractive index mismatch and monomer reactivity influence composite curing depth. J Dent Res 2008;87(1):84–8. https://doi.org/10.1177/154405910808700115.

[18] Santos C, Luklinska ZB, Clarke RL, Davy KWM. Hydroxyapatite as a filler for dental composite materials: mechanical properties and in vitro bioactivity of composites. J Mater Sci: Mater Med 2001;12(7):565–73. https://doi.org/10.1023/A:1011291723503.

[19] Arcis RW, Lopez-Macipe A, Toledano M, Osorio E, Rodriguez-Clemente R, Murtra J, et al. Mechanical properties of visible light-cured resins reinforced with hydroxyapatite for dental restoration. Dent Mater 2002;18(1):49–57. https://doi.org/10.1016/s0109-5641(01)00019-7.

[20] Walker CS, Sutou S, Oda C, Mihara M, Honda A. Calcium silicate hydrate (C-S-H) gel solubility data and a discrete solid phase model at 25°C based on two binary non-ideal solid solutions. Cem Concr Res 2016;79:1–30. https://doi.org/10.1016/j.cemconres.2015.07.006.

[21] Prati C, Gandolfi MG. Calcium silicate bioactive cements: biological perspectives and clinical applications. Dent Mater 2015;31(4):351–70. https://doi.org/10.1016/j.dental.2015.01.004.

[22] Park SH, Ye JR, Asiri NM, Chae YK, Choi SC, Nam OH. Biocompatibility and bioactivity of a dual-cured resin-based calcium silicate cement: in vitro and in vivo evaluation. J Endod 2024;50(2):235–42. https://doi.org/10.1016/j.joen.2023.11.009.

[23] Gandolfi MG, Taddei P, Siboni F, Modena E, De Stefano ED, Prati C. Biomimetic remineralization of human dentin using promising innovative calcium-silicate hybrid "smart" materials. Dent Mater 2011;27(11):1055–69. https://doi.org/10.1016/j.dental.2011.07.007.

[24 Formosa LM, Mallia B, Camilleri J. The chemical properties of light- and chemical-curing composites with mineral trioxide aggregate filler. Dent Mater 2013;29(2):e11–9. https://doi.org/10.1016/j.dental.2012.11.006.

[25] Chung H, Kim M, Ko H, Yang W. Evaluation of physical and biologic properties of the mixture of mineral trioxide aggregate and 4-META/MMA-TBB resin. Oral Surg Oral Med Oral Pathol Oral Radiol Endodontol 2011;112(5):e6–11. https://doi.org/10.1016/j.tripleo.2011.04.005.

[26] Chiari MD, Rodrigues MC, Xavier TA, de Souza EM, Arana-Chavez VE, Braga RR. Mechanical properties and ion release from bioactive restorative composites containing glass fillers and calcium phosphate nano-structured particles. Dent Mater 2015;31(6):726–33. https://doi.org/10.1016/j.dental.2015.03.015.

[27] Vilela HS, Campos AL, Cabral C, Chiari MDS, Vieira DN, Braga RR. Effect of calcium orthophosphate: Reinforcing glass ratio and prolonged water storage on flexural properties of remineralizing composites. J Mech Behav Biomed Mater 2020;104:103637. https://doi.org/10.1016/j.jmbbm.2020.103637.

[28] Rosenstiel SF, Johnston WM. The effects of manipulative variables on the color of ceramic metal restorations. J Prosthet Dent 1988;60(3):297–303. https://doi.org/10.1016/0022-3913(88)90272-7.

[29] Chung SM, Yap AU, Koh WK, Tsai KT, Lim CT. Measurement of Poisson's ratio of dental composite restorative materials. Biomaterials 2004;25(13):2455–60. https://doi.org/10.1016/j.biomaterials.2003.09.029.

[30] Johnston WM. Review of translucency determinations and applications to dental materials. J Esthet Restor Dent 2014;26(4):217–23. https://doi.org/10.1111/jerd.12112.

[31] Oh HJ, Lee CH, Lee IB. Real-time measurement of transmittance changes during photo-polymerization of conventional and bulk-fill composites. Dent Mater J 2022;41(6):800–7. https://doi.org/10.4012/dmj.2022-009.

[32] Ruyter IE, Oysaed H. Conversion in different depths of ultraviolet and visible light activated composite materials. Acta Odontol Scand 1982;40(3):179–92. https://doi.org/10.3109/00016358209012726.

[33] Naganuma T, Kagawa Y. Effect of particle size on light transmittance of glass particle dispersed epoxy matrix optical composites. Acta Mater 1999;47(17):4321–7. https://doi.org/10.1016/S1359-6454(99)00329-8.

[34] Trinca RB, Oliveira BA, Vilela HDS, Braga RR. Effect of calcium orthophosphate particle size and CaP:glass ratio on optical, mechanical and physicochemical characteristics of experimental composites. Dent Mater 2023. https://doi.org/10.1016/j.dental.2023.06.012.

[35] Feng L, Suh BI, Shortall AC. Formation of gaps at the filler-resin interface induced by polymerization contraction stress: Gaps at the interface. Dent Mater 2010;26(8):719–29. https://doi.org/10.1016/j.dental.2010.03.004.

[36] Sideridou I, Tserki V, Papanastasiou G. Effect of chemical structure on degree of conversion in light-cured dimethacrylate-based dental resins. Biomaterials 2002;23(8):1819–29. https://doi.org/10.1016/s0142-9612(01)00308-8.

[37] Arcis RW, Lopez-Macipe A, Toledano M, Osorio E, Rodriguez-Clemente R, Murtra J, et al. Mechanical properties of visible light-cured resins reinforced with hydroxyapatite for dental restoration. Dent Mater 2002;18(1):49–57. https://doi.org/10.1016/s0109-5641(01)00019-7.

[38] Skrtic D, Antonucci JM. Effect of bifunctional comonomers on mechanical strength and water sorption of amorphous calcium phosphate- and silanized glass-filled Bis-GMA-based composites. Biomaterials 2003;24(17):2881–8. https://doi.org/10.1016/s0142-9612(03)00119-4.

[39] Arita K, Yamamoto A, Shinonaga Y, Harada K, Abe Y, Nakagawa K, et al. Hydroxyapatite particle characteristics influence the enhancement of the mechanical and chemical properties of conventional restorative glass ionomer cement. Dent Mater J 2011;30(5):672–83. https://doi.org/10.4012/dmj.2011-029.

[40] Tanimoto Y, Kitagawa T, Aida M, Nishiyama N. Experimental and computational approach for evaluating the mechanical characteristics of dental composite resins with various filler sizes. Acta Biomater 2006;2(6):633–9. https://doi.org/10.1016/j.actbio.2006.06.006.

[41] Griffith AA. The phenomena of rupture and flow in solids. Philos Trans R Soc A: Math, Phys Eng Sci 1921;221:35 (Doi:).

[42] Shah PK, Stansbury JW. Role of filler and functional group conversion in the evolution of properties in polymeric dental restoratives. Dent Mater 2014;30(5):586–93. https://doi.org/10.1016/j.dental.2014.02.015.

[43] Xu HHK, Weir MD, Sun L. Nanocomposites with Ca and PO4 release: Effects of reinforcement, dicalcium phosphate particle size and silanization. Dent Mater 2007;23(12):1482–91. https://doi.org/10.1016/j.dental.2007.01.002.

[44] Trinca RB, Vela BF, dos Santos Vilela H, Braga RR. Ion release mechanisms in composites containing CaP particles and hydrophilic monomers. Dent Mater 2024;40(7):1047–55. https://doi.org/10.1016/j.dental.2024.05.008.

[45] Xu HH, Weir MD, Sun L. Nanocomposites with Ca and PO4 release: effects of reinforcement, dicalcium phosphate particle size and silanization. Dent Mater 2007;23(12):1482–91. https://doi.org/10.1016/j.dental.2007.01.002.
[46] Gallo M, Le Gars Santoni B, Douillard T, Zhang F, Gremillard L, Dolder S, et al. Effect of grain orientation and magnesium doping on beta-tricalcium phosphate resorption behavior. Acta Biomater 2019;89:391–402. https://doi.org/10.1016/j.actbio.2019.02.045.
[47] Dickens SH, Flaim GM. Effect of a bonding agent on in vitro biochemical activities of remineralizing resin-based calcium phosphate cements. Dent Mater 2008;24(9):1273–80. https://doi.org/10.1016/j.dental.2008.02.004.